Kochi Chapter

Indian Geotechnical Conference
IGC 2022
15th – 17th December, 2022, Kochi

Application of Multilaminate Model to Analyse the Influence of Principal Stress Rotation Stress Paths on Permanent Deformation of Railway Ballast

Rakesh Sai Malisetty[1*], Buddhima Indraratna[1] and Jayan S. Vinod[2]

[1] Transport Research Centre, School of Civil and Environmental Engineering, University of Technology Sydney, Australia
[2] University of Wollongong, Australia
*rakeshsai.malisetty@uts.edu.au

Abstract. Moving trains cause significant amplification of dynamic stresses in the shallow track layers. Under these stresses, railway ballast undergoes exacerbated permanent deformation and degradation that will eventually increase the maintenance costs of railway track. In addition to stress amplification, stress paths are also affected by moving train loads due to the rotation of principal stress axes. In this paper, the influence of different principal stress rotation (PSR) stress paths on permanent deformation response of ballast are analysed using a multilaminate constitutive model. The constitutive model is calibrated and validated with the laboratory tests on ballast under triaxial compression stress paths and extended to PSR stress paths. The PSR stress paths are quantified using a new modified cyclic stress ratio (CSR*) which incorporates the effects of both load amplification and principal stress rotation. The model predictions show that permanent deformations increase with CSR* and vary with changes in stress path even when cyclic loading amplitude remains constant. When PSR stress paths are considered, the permanent deformations amplify at a higher rate than for the cases without PSR. Further, the shakedown response of permanent deformations under PSR stress paths is investigated based on the model predictions.

Keywords: railway ballast, principal stress rotation, multilaminate model

1 Introduction

Railway track substructure plays a vital role in determining the safety and performance of railway networks in a country. One of the critical components of track substructure, ballast layer absorbs most of the kinetic energy exerted by moving trains and provides necessary load bearing. Several studies are available in literature explaining the laboratory behavior of ballast under railway loading [1-4]. Some key driving factors that affect deformations in ballast layer include the magnitude of axle loads, loading frequency and the effective confining stress. In addition to the above-mentioned factors, principal stress rotation (PSR) and dynamic amplification of vertical stresses also affect the deformation of ballast especially in the context of high-speed passenger trains or medium speed freight trains. Under moving loads, the stress paths in the shallow substructure layers become complex with the rotation of principal stresses and dynamic

vertical stress amplification. Also, these stress paths change their shape and magnitude with different train speeds, axle loads and the underlying ground conditions. Through mathematical and numerical models [5-7], it was reported that the rotation of principal stress axes affects the effective stress paths that the ballast layer will be subjected to under moving train loads.

Laboratory simulation of principal stress rotation for coarse granular materials has practical limitations with the size and sophistication of machinery required. Studies on soft subgrade clays and fine sands showed that the permanent axial strain response of the material is amplified under principal stress rotation and the material becomes unstable under PSR stress paths with higher shear stresses. In this context, Malisetty et. al.[8] proposed a constitutive model based on multi-laminate framework that can capture the behavior of ballast under a wide range of stress paths: from complex PSR stress paths to simple triaxial compression stress paths. In this paper, the multi-laminate constitutive model is used to analyse the influence of different principal stress rotation stress paths on the permanent axial deformation behavior of ballast. A brief description of multi-laminate framework is presented followed by its application to railway ballast under moving load stress paths.

2 Multi-laminate constitutive model

In multi-laminate framework, the granular matrix is assumed to consist of multiple contact planes that can be grouped into a finite number of orientations, where the global stress state is transformed into mesoscopic stress state as shown in Fig.1. The overall macroscopic strain response of the granular matrix under loading can be represented as the sum of meso-scale responses at the inter-particle contact planes [9]. By considering the meso-scale stress-deformation response, the effects of stress-induced anisotropy are captured inherently within the model.

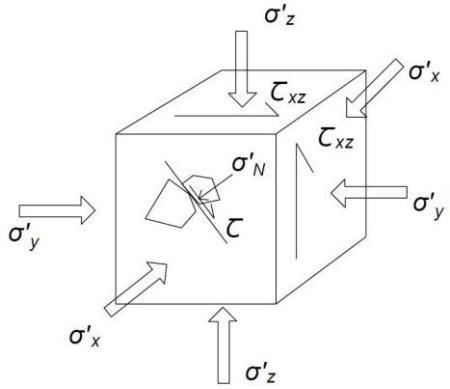

Fig. 1. Conceptualization of multi-laminate framework

Under a 3D global stress state, the meso-scale stresses at the contact planes can be written as:

$$\sigma_m = T_m . \sigma'_{iiii} \quad (1)$$

where, $\sigma_{iiii} = [\sigma_x \quad \sigma_y \quad \sigma_z \quad r_{xy} \quad r_{yz} \quad r_{zx}]$, $\sigma_m' = \begin{pmatrix} \sigma_N' \\ r \end{pmatrix}$ and T_m is the transformation matrix on the m^{th} contact plane. The components of T_m are represented as the partial derivatives of normal and shear stresses on the plane with the global stresses given by:

$$T_m = \begin{pmatrix} \frac{\partial \sigma_N^F}{\partial \sigma_x^F} & \frac{\partial \sigma_N^F}{\partial \sigma_y^F} & \frac{\partial \sigma_N^F}{\partial \sigma_{zz}^F} & \frac{\partial \sigma_N^F}{\partial c_{xy}} & \frac{\partial \sigma_N^F}{\partial c_{yzz}} & \frac{\partial \sigma_N^F}{\partial c_{zx}} \\ \frac{\partial c}{\partial \sigma_x^F} & \frac{\partial c}{\partial \sigma_y^F} & \frac{\partial c}{\partial \sigma_{zz}^F} & \frac{\partial c}{\partial c_{xy}} & \frac{\partial c}{\partial c_{yzz}} & \frac{\partial c}{\partial c_{zx}} \end{pmatrix} \quad (2)$$

The overall incremental stress-strain relationship can be given by:

$$\partial\sigma'_{iiii} = \frac{1}{C^e} \partial\varepsilon^e + \sum_{m=1} T_m \, \partial\varepsilon_m^p \, w_m \quad (3)$$

where, C^e is the elastic compliance matrix, $\partial\varepsilon^e$ represent the incremental global elastic strain matrix, $\partial\varepsilon_m^p$ is the local plastic strain matrix at m^{th} contact plane, M is the total number of contact plane orientations and w_m is the weighting coefficient on the m^{th} plane.

2.1 Constitutive relationships

The mechanical behavior of railway ballast is affected by the breakage of angular asperities resulting in a nonlinear critical state. Based on recent investigations [10], the critical state friction angle on the m^{th} plane ($\emptyset'_{cm}$) can be represented as a function of Ballast Breakage Index (BBI) as:

$$\emptyset'_{cm} = \tan^{-1}(tan(\emptyset_{c0}) \, exp(-aBBI_m)) \quad (4)$$

$$BBI_m = \frac{b_1}{b_3 - \ln\left(\frac{P_0^F}{P_a^F}\right)} \left(1 - \exp\left(-b_2 \gamma^p_m\right)\right) \quad (5)$$

The critical state line (CSL) in $v - \ln p'$ space is given by:

$$v = 1 + e_{rerr} - bexp(cBBI) - \lambda_c \ln p' \quad (6)$$

where, v is the specific volume, a, b, c, b_1, b_2, b_3 are breakage parameters, p'_0 is the initial confining stress on the material and λ_c is the slope of the CSL in the $v - lnp'$ space.

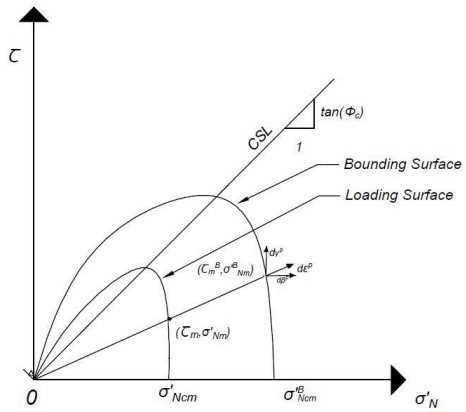

Fig. 2. Breakage-dependent bounding surface for ballast (modified after Malisetty, et. al. [8])

For establishing the stress-strain relationships, a breakage dependent bounding and yield surfaces are developed as shown in Fig.2 and can be given as:

$$F_m = r^B_{m\,cm} - \tan\emptyset' \left(\frac{\gamma\gamma^p_m}{A_h + \gamma\gamma_m} \right) \left(\frac{\ln\left(\frac{\sigma^{FB}_{Nmc}}{\sigma^{FB}_{Nm}}\right)}{\ln R} \right)^{\frac{1}{y}} \sigma'^B_{Nm} = 0 \quad (7)$$

$$f_m = r_m - \tan\emptyset'_{cm} \left(\frac{\gamma\gamma^p_m}{A_h + \gamma\gamma_m} \right) \left(\frac{\ln\left(\frac{\sigma^F_{Nmc}}{\sigma^F_{Nm}}\right)}{\ln R} \right)^{\frac{1}{y}} \sigma'_{Nm} = 0 \quad (8)$$

where, A_h is a model parameter, R and y are the bounding surface shape parameters and the suffix B denotes the corresponding stress vectors on the bounding surface which are determined through radial mapping rule. Dilatancy in multi-laminate framework is represented at the meso-scale by taking the ratio of incremental plastic strains in normal $\partial\partial\beta^p_m$ and shear $\partial\partial\gamma^p_m$ directions, respectively and can be represented as a function of changes in void ratio as:

$$ddd_m = \frac{\partial\partial\beta^p_m}{\partial\partial\gamma^p_m} = k_d(1 + d_2 ff)\left(\exp\left(d_1(e - e_c)\right) - \frac{y_m}{\tan\emptyset_c}\right) \quad (9)$$

where, k_d, d_1, d_2 are the material constants, ff is the loading frequency and $\gamma\gamma_m$ is the stress ratio on the m^{th} plane. In Eq.9, d_2 captures the effect of loading frequency on increased dilatancy of the material.

The incremental strains can be given by:

$$\partial\partial\beta^p_m = dL_m \frac{\partial\partial g_m}{\partial\partial\sigma^F_{Nm}}; \partial\partial\gamma^p_m = dL_m \frac{\partial\partial g_m}{\partial\partial c_m} \quad (10)$$

where, $g_m = r_m - ddd_m\sigma'_{Nm}$ is the plastic potential function and dL_m is the plastic multiplier which is a function of plastic hardening modulus, that controls the magnitude of plastic strains. More details of the characteristics of bounding surface, plastic hardening modulus and derivation of hardening rule are given in [8].

2.2 PSR stress paths under moving loads

When a train passes over a railway track, the principal stresses in the soil element experiences rotation predominantly in the longitudinal direction, i.e., in the direction of passage of the train. Considering x, y, z as longitudinal, lateral and vertical directions respectively, the resulting stress paths can be best represented in in the $r_{xz} - (\sigma'_z - \sigma'_x)$ stress space as shown in Fig.3. Tucho et al. [6] reported that in railway tracks, these stress paths under a moving train attain a cardioid shape and are selected for analysis in this study. It is to be noted that in PSR stress paths, the stress state continuously changes from triaxial compression to pure shear stress state in each cycle. The size of the cardioid shape stress paths is quantified using a modified Cyclic Stress Ratio (CSR*) given by:

$$\text{CSR*} = CSR\sqrt{1 + 4SSR^2} \quad (11)$$

where, CSR = $\frac{\Delta(\sigma^F_z - \sigma^F_x)_{cyc}}{2\sigma^F_{yy}}$ and SSR = $\frac{\tau^F_{xz,cyc}}{(\sigma^F_z - \sigma^F_x)_{cyc}}$

CSR is the cyclic stress ratio which is used widely in analyzing the vertical stress effects on railway substructure materials under triaxial compression conditions, while Shear Stress Ratio (SSR) captures the effect of shear stresses that are developed due to moving loads. When the loading occurs predominantly in the vertical direction, SSR becomes 0 and CSR* reduces to CSR.

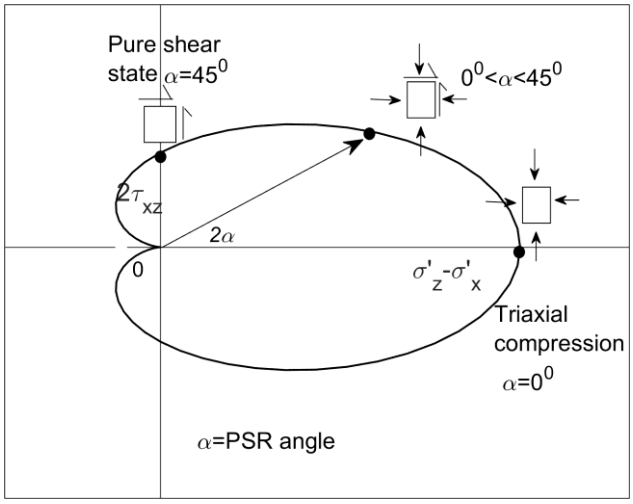

Fig. 3. Visualization of PSR stress path in $r_{xz} - (\sigma_z^{'} - \sigma_x^{'})$ space

3 Predicted deformation behavior

The multi-laminate constitutive model is used to predict the deformation behavior of ballast under cyclic loading with and without principal stress rotation. The material parameters used in this study are categorized into 5 types: shear modulus and Poisson's ratio (G, $\nu\nu$), critical state parameters ($\emptyset_{c0}^{'}$, λ_c, k, e_{rerr}, a, b, c, b_1, b_2, b_3), dilatancy parameters (k_d, d_1, d_2), bounding surface (R, y) and hardening parameters (A_h, α_s), and are shown in Table-1. Determination of each of these parameters from laboratory data are given in Malisetty et. al. [8]. For numerical integration in multi-laminate framework, 26 different plane orientations with their weight coefficients are considered as given in Malisetty et. al. [8].

Table 1 Ballast parameters in multi-laminate constitutive model

	Elastic parameters	Critical state parameters	Dilatancy parameters	Bounding surface parameters	Hardening parameters
Value	G=10MPa $\nu\nu$=0.3	$\emptyset_{c0}^{'}$= 56^0 λ_c =0.095 k =0.007 e_{rerr} =1.41 a =0.2 b = 1.87 c = 1.86 b_1 = 0.25 b_2 = 2 b_3= 6.4	k_d= 0.35 d_1= 0.2 d_2= 0.005	R=10 y=5	A_h=0.01 α_s=20

3.1 Behavior under triaxial compression stress paths

Figure 4 shows the validation of model predictions with laboratory data from different studies on ballast under various cyclic loading conditions [11, 12]. For the different loading conditions considered, the corresponding CSR values are shown in Fig.4 and since these tests were performed under triaxial compression conditions, SSR is kept equal to 0. The permanent axial strains increase rapidly in the first 1000 cycles and then reach a stable shakedown state, where no further increment is observed. The model can capture the reduction of permanent axial strains at shakedown state with increasing confining stress from 60 kPa to 120 kPa. This is because an increase in confining stress of the material increases the shear strength of the material. The effect of loading frequency is simulated by increasing the CSR due to dynamic stress amplification and the model captures the resulting amplification of permanent axial strains very well. Further, it can be consistently observed that as CSR increases, the permanent axial strains also increase irrespective of confining stress and loading frequency.

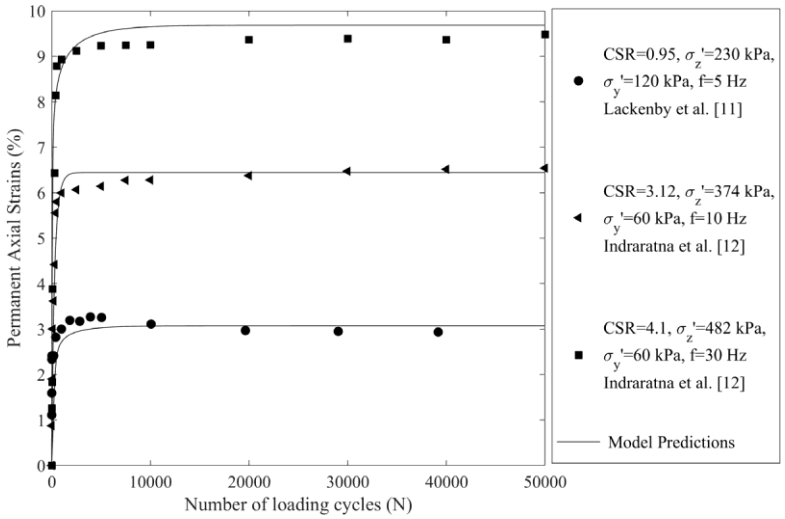

Fig. 4. Permanent axial strain response of ballast under cyclic triaxial compression conditions predicted by multi-laminate constitutive model (reproduced from Malisetty et al. [8])

3.2 Influence of PSR stress paths

The model is used to predict the permanent axial strain response of ballast under principal stress rotation stress paths and same model parameters as in Table-1 are used. For analyzing the influence of principal stress rotation stress paths, the stress paths were quantified in terms of shear stress ratio (SSR) and SSR is varied for two values of CSR, for a confining stress (σ_y') of 30 kPa was used. From Fig.5, it can be observed that the when CSR is kept constant at 3.83 (solid lines), increase in SSR increased the magnitude of permanent axial strains, signifying the influence of principal stress rotation and the resulting stress induced anisotropy on the material response. For higher CSR value of 4.5 (dotted lines), the magnitude of predicted axial strains for a particular SSR

increase when compared to similar SSR value for CSR=3.83. Further, the amplification of permanent axial strains with SSR is higher for CSR=4 when compared to that of 3.83. As SSR is increased, the tendency of the material to reach shakedown state reduced and for the case of CSR=4 and SSR=0.4, the material showed plastic ratcheting state where rapid increment of axial strains is expected.

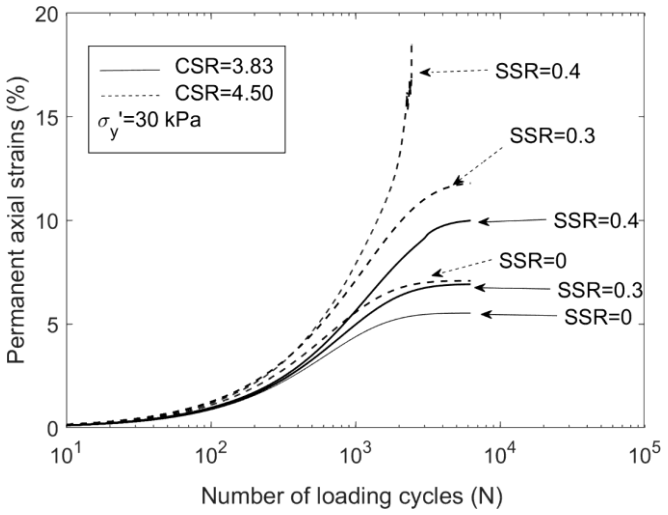

Fig. 5. Influence of CSR and SSR on permanent axial strain response – Multilaminate constitutive model predictions (data sourced from Malisetty et. al. [8])

Fig.6. shows the magnitude of permanent axial strain when the material reached shakedown by converting CSR and SSR into an equivalent CSR*. It can be observed that the permanent axial strains follow a non-linear amplification trend with increasing CSR* values and after a particular CSR* range, the predictions show that material did not reach shakedown state and showed an unstable plastic ratcheting response eventually reaching failure. This CSR* at which the material becomes unstable can be considered as the critical modified cyclic stress ratio, which is found from this study as 5.8. Considering the slope of the axial strain vs CSR* curve, linear trend lines can be drawn and three distinct zones are identified including stable, metastable and unstable zones as shown in Fig.6. In the unstable zone, the material experiences plastic ratcheting and no data point corresponding to the plastic shakedown state.

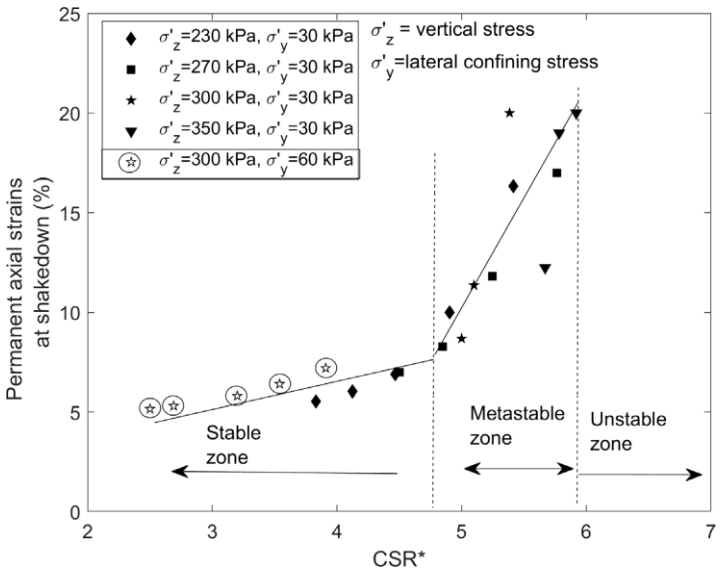

Fig. 6. Influence of CSR* on permanent axial strains of ballast at shakedown

3.3 Effect of confining stress

Many earlier studies reported that the strength of granular materials is dependent on the effective confining stress of the material. Higher confining stresses lead to higher shear strength of the material and increased compression. However, an important parameter for coarse granular materials such as ballast, particle breakage follows a different trend when compared to the shear strength and is minimum in the confining stress range of 40 to 60 kPa. It is also observed from the current analysis that for the same axle load (vertical stress, σ_z'=300 kPa), increasing the confining stress from 30 kPa to 60 kPa makes the material more stable (see Fig.6) as the permanent axial deformations reduce.

In the real field conditions, this increased confining stress can be achieved through different track interventions or design modifications [13]. These include modified winged sleepers and lateral restraints using containing sheets which prevent ballast on the shoulders to move laterally outward, thus increasing the confining stress. In addition, the use of geogrids to reinforce ballast was also proven to increase the shear strength of ballast by improving the particle interlock and increasing the ballast friction angle.

4 Conclusions

In this paper, a new constitutive model for ballast developed using multi-laminate framework is presented. The constitutive equations are developed based on the breakage-dependent non-linear critical state behavior of ballast observed in laboratory. The model performance showed that the multi-laminate framework can simulate the influence of PSR stress paths that are observed under moving train loads on the deformation of ballast. It was found that increasing both CSR and SSR increased permanent axial

strains and reduced the stability of ballast. Increasing magnitudes of CSR and SSR led to the amplification of permanent axial strains at shakedown and after certain magnitudes, the material does not reach shakedown and show ratcheting response. The shakedown axial strains showed a non-linear trend with a modified cyclic stress ratio (CSR*), through which three distinct zones can be determined based on the amplification of shakedown axial strains.

While the traditional triaxial compression type analysis only consider the influence of vertical stress (CSR) on the permanent deformations, this study showed even when vertical stresses remain the same, increasing SSR can itself lead to exacerbating deformations. This study also highlights the need to consider the influence of PSR stress paths and CSR* while improving railway tracks for high speed passenger or medium speed heavy haul trains in future.

Acknowledgements

The authors would like to acknowledge the financial assistance provided by the Australian Research Council Industrial Transformation Training Centre for Advanced Technologies in Rail Track Infrastructure (ITTC-Rail: IC170100006).

References

1. Indraratna, B., J. Lackenby, and D. Christie, Effect of confining pressure on the degradation of ballast under cyclic loading. Géotechnique, 2005. **55**(4): p. 325-328.
2. Sun, Q., B. Indraratna, and S. Nimbalkar, Effect of cyclic loading frequency on the permanent deformation and degradation of railway ballast. Géotechnique, 2015. **64**(9): p. 746-751.
3. Suiker, A.S., E.T. Selig, and R. Frenkel, Static and cyclic triaxial testing of ballast and subballast. ASCE Journal of Geotechnical and Geoenvironmental Engineering, 2005. **131**(6): p. 771-782.
4. Thakur, P.K., J.S. Vinod, and B. Indraratna, Effect of confining pressure and frequency on the deformation of ballast. Géotechnique, 2013. **63**(9): p. 786-790.
5. Yang, L., W. Powrie, and J. Priest, Dynamic stress analysis of a ballasted railway track bed during train passage. ASCE Journal of Geotechnical and Geoenvironmental Engineering, 2009. **135**(5): p. 680-689.
6. Tucho, A., B. Indraratna, and T. Ngo, Stress-deformation analysis of rail substructure under moving wheel load. Transportation Geotechnics, 2022. **36**: p. 100805.
7. Bian, X., et al., Analysing the effect of principal stress rotation on railway track settlement by discrete element method. Géotechnique, 2019: p. 1-19.
8. Malisetty, R.S., B. Indraratna, and J. Vinod, Behaviour of ballast under principal stress rotation: Multi-laminate approach for moving loads. Computers and Geotechnics, 2020. **125**: p. 103655.
9. Zienkiewicz, O. And G. Pande, Time-dependent multilaminate model of rocks—a numerical study of deformation and failure of rock masses. International Journal for Numerical and Analytical Methods in Geomechanics, 1977. **1**(3): p. 219-247.

10. Indraratna, B., Q.D. Sun, and S. Nimbalkar, Observed and predicted behaviour of rail ballast under monotonic loading capturing particle breakage. Canadian Geotechnical Journal, 2015. **52**(1): p. 73-86.
11. Lackenby, J., et al., Effect of confining pressure on ballast degradation and deformation under cyclic triaxial loading. Géotechnique, 2007. **57**(6): p. 527-536.
12. Indraratna, B., P.K. Thakur, and J.S. Vinod, Experimental and numerical study of railway ballast behavior under cyclic loading. International Journal of Geomechanics, 2010. **10**(4): p. 136-144.
13. Indraratna, B., et al., Ballast characteristics and the effect of geosynthetics on Rail track deformation, in International Conference on Geosynthetics and Geoenvironmental Engineering. 2004, Quest Publications: Bombay. P. 3-12.